ChemComm

COMMUNICATION

View Article Online
View Journal | View Issue

Cite this: *Chem. Commun.*, 2025, **61**, 7648

Received 16th February 2025,
Accepted 21st April 2025

DOI: 10.1039/d5cc00857c

rsc.li/chemcomm

Preparation of electrochemical aptamer-based sensors: a direct aryl diazonium grafting approach†

Essam M. Dief,[a] Wenxian Tang,[a] Liam R. Carroll,[a] Tony Breton *[b] and J. Justin Gooding *[a]

Electrochemical aptamer-based (EAB) sensors represent a promising platform for continuous monitoring of a wide range of biomarkers due to the unique properties of aptamers, such as high affinity, target binding reversibility and ease of designing them for a desired target analyte. Currently, the performance of EAB sensors is limited by the instability of the molecule/electrode link that is mostly based on the gold–sulphur semi-covalent bonds that can be chemically and electrochemically unstable during operation of an EAB sensor. In this work, we introduce, for the first time, an aryl diazonium salt-derived covalent surface chemistry that enables the direct grafting of aptamers on gold electrodes, in a single step, by the spontaneous reduction of an *in situ* diazotized aryl-aminated aptamer derivative. This method allows for more robust attachment of aptamers on gold electrodes *via* the formation of a more stable interfacial gold–carbon bond. The fabricated sensor shows a capability to continuously monitor the antibiotic vancomycin target in phosphate-buffered saline (PBS) solution for over 48 hours. This work opens new avenues to overcome the instability related to thiol–gold chemistry for the development of EAB sensors in wearable devices.

Developing a continuous monitoring platform for many chemical and biochemical analytes in real time in complex biofluids is the ultimate yet to be realised goal in sensing.[1,2] This would ideally require the biorecognition element to possess certain features such as high affinity to targets, binding reversibility, selectivity and capability of being tailored to detect multiple different targets. With all the great progress in the sensing and the biosensing space over the past century, from developing continuous glucose monitors[3,4] to high affinity immunoassays,[5] finding a biorecognition element that meets the criteria for continuous monitoring remained elusive until the discovery of aptamers – nucleic acid molecules that can reversibly bind to various targets depending on the sequence of the nucleic acid and its structure.[6] By combining the discovery of aptamers and the knowledge from the earlier-developed nucleic acid electrochemical biosensors,[7,8] Plaxco and co-workers developed electrochemical aptamer-based (EAB) sensors as a promising platform for continuous monitoring that has been shown to be capable of continuously monitoring drug levels *in vivo*.[9,10] Despite the fascinating potential of EAB sensors, the platform is still facing some challenges with the interface instability representing a bottleneck for their long-term performance in complex biological media.[11]

An EAB sensor is typically composed of a single-stranded aptamer DNA that is functionalised with an alkanethiol at the proximal end of the aptamer and a redox probe (*e.g.*, methylene blue) at the distal end.[12,13] When no analytical target is present in the biological sample, the tethered redox probe can move freely above the electrode surface. Accompanying the aptamer on the surface is a diluent mercaptohexanol (MCH), which serves to ensure that the DNA aptamer does not lie flat on the gold.[9,14] Binding the aptamer to the target molecule confines the redox probe closer to the surface, which thus leads to an increase in the rate of electron transfer with a concomitant increase in current.[12,15] The change in the electron transfer rate is proportional to the concentration of the target molecule in the sample. In addition to the redox-labelled EAB sensor architecture, a redox label-free configuration has been developed where the signal transduction involves a redox process of redox coupled ions in solution. While redox-labelled EAB sensors are more sensitive and suitable for real-time continuous measurements compared to label-free aptamer sensors, the presence of a redox probe connected to the aptamer causes faster sensor degradation due to the potential interrogation that might accelerate the Au–S bond degradation.[16] Moreover, methylene blue is pH sensitive and that might cause sensing variations and instability when deployed in biological fluids.[17]

[a] *School of Chemistry and Australian Centre for NanoMedicine, University of New South Wales, Sydney, New South Wales, Australia. E-mail: justin.gooding@unsw.edu.au*
[b] *Univ Angers, CNRS, MOLTECH-Anjou, SFR MATRIX, F-49000 Angers, France. E-mail: tony.breton@univ-angers.fr*

† Electronic supplementary information (ESI) available. See DOI: https://doi.org/10.1039/d5cc00857c

Both the ease of assembly and the control over the final aptamer/MCH interface when using alkanethiol monolayers spontaneously assembled on gold are key to the success of the EAB concept; however, the long-term stability of these sensing interfaces is a challenge for advancing the technology. The desorption of the alkanethiol monolayers occurs when the gold–thiolate bond oxidises[18] and when sufficient energy is applied to the system.[19] Therefore, finding a more robust alternative to the Au–S interfacial bond, either *via* replacing the electrode substrate or molecular anchoring, could potentially play an important role in moving this technology forward.

Other surface chemistry approaches such as the use of pyrenes[20] and its analogues to connect nucleic acids to graphene electrode substrates in the graphene field effect transistor (GFET) architecture *via* π–π stacking.[21,22] The GFET was then coated with an antifouling membrane and the sensor retained its signal for a few days. Although the pyrene-enabled GFET sensor showed good stability in biofluids, that stability might be attributed to the presence of the antifouling layer. There are some concerns regarding the physical displacement and the resistance of this physisorption-based anchoring chemistry to continuous potential interrogation.[11,21] Phosphates on ITO have also been exploited to fabricate EAB sensors but the sensors were found to be less stable than the alkanethiol ones, and the instability was attributed to the instability of the underlying ITO material rather than the surface chemistry itself.[23]

Molecular contacts such as carbon–gold covalent bonds have shown higher stability in molecular devices,[24,25] but endeavours to replace the Au–S bond by a carbon-based anchoring on electrodes have been unsuccessful so far, mainly because of the challenging control of the radical chemistry involved and the subsequent aptamer attachment, which lead to the absence of aptamer organization on the surface, and possibly to multilayer formation. An example using the aryl diazonium chemistry, from which we draw inspiration,[26] involved modifying the glassy carbon electrode with an aryl diazonium salt or an aliphatic amine layer and then in a second step attaching the aptamer. Despite this elegant chemistry, only EAB sensors with an electrochemically grafted aliphatic amine monolayer were found to be more stable compared to the common thiol–gold based ones. The authors also highlighted that the aryl diazonium layer-based sensors showed no response,[26] which was attributed to the possibility of low control over the aryl diazonium reduction process in the underlying layer, the presence of physically adsorbed species and the tendency for forming multilayers.[27,28] In contrast to the previous multistep strategies for forming EAB sensors using aryl diazonium salt layers, herein we present a completely new way of forming these layers in a single one-step strategy that potentially gives greater control over the sensing interface.

The spontaneous grafting of an aptamer on gold reported here involved an aptamer DNA functionalized with 4-aminobenzoic acid (4-ABA) at one end (5′ terminal) and a methylene blue moiety at the other end (3′ terminal). The NH_2 group of the 4-ABA can undergo diazotization *via* the addition of sodium nitrite ($NaNO_2$) as a diazotizing agent in the presence of hydrochloric acid (HCl). The obtained aryl diazonium terminated aptamer spontaneously decomposed at the gold interface into the corresponding aryl radicals, which subsequently grafted to the metal.[29] The sensing response of the generated interface was tested in the presence of different concentrations of the antibiotic drug vancomycin in phosphate-buffered saline (PBS) and the fabricated sensors were used in continuous monitoring of vancomycin in PBS buffer.

Fig. 1a shows a schematic depicting the utilised surface chemistry that involves *in situ* diazotization and subsequent spontaneous reduction at the gold-solution interface, leading to the grafting of the aryl radicals produced. The electrochemical response of the methylene blue probe was recorded using square wave voltammetry (SWV) in PBS solution confirming the attachment of the functionalized aptamer on the gold electrode (Fig. 1b). After the addition of 20 μM of vancomycin, an increase of the SWV signal can be observed (Fig. 1b). This positive response in current can be explained by the target binding-induced conformational change in the aptamer structure, which accelerates electron transfer from methylene blue to the gold electrode, presumably by the methylene blue becoming closer to the electrode surface upon target binding.[9,30] Although the increase in current is not as great

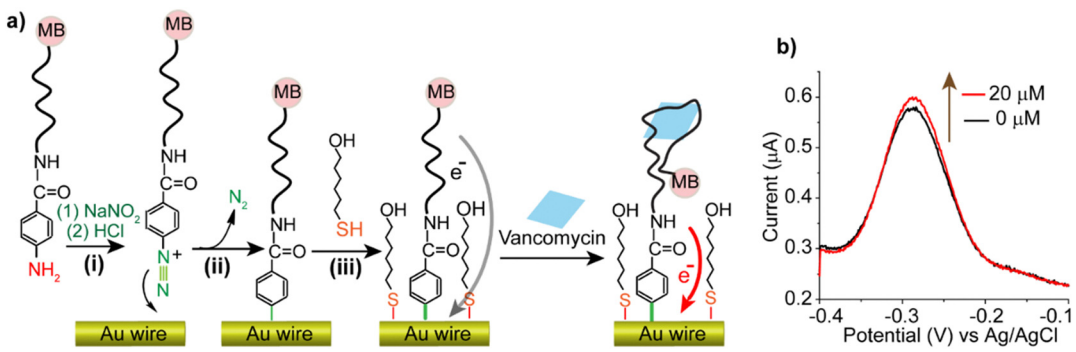

Fig. 1 (a) Reaction sequence followed for the grafting of the aptamer used for vancomycin detection *via* the *in situ* generation of its aryl diazonium derivative and subsequent backfilling of the surface by adsorption of 6-mercapto-1-hexanol (MCH). (b) Square wave voltammograms recorded at 150 Hz in the absence and after the addition of 20 μM of vancomycin.

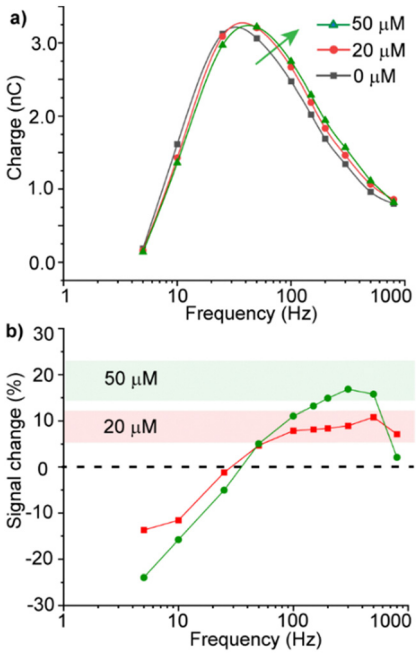

Fig. 2 (a) Evolution of the aryl diazonium EAB sensor charge obtained from square wave voltammetry at different frequencies before and after vancomycin addition. (b) Change in the signal gain recorded in the same frequency range after vancomycin addition.

as that observed with the same aptamer bonding to gold *via* alkanethiol chemistry,[12,31] the signal increase is consistent with the presence of functional aptamers on the surface. Such results demonstrate that the aryl diazonium strategy can be used to attach modified aptamers, with the covalent bond formation not hindering interactions with the target. To further understand the kinetics of the aptamer response, square wave voltammograms were recorded at frequencies ranging from 5 Hz to 1000 Hz in the absence and in the presence of increasing concentrations of vancomycin. The charge–frequency plot presented in Fig. 2a shows the electrochemical response of the methylene blue probe as a function of the SWV frequency used to interrogate the sensing interface. Without vancomycin, the signal showed a maximum at 33 Hz. After the addition of 20 and then 50 μM of vancomycin, the charge–frequency plot was shifted towards higher frequencies, which indicates an increase of the electron transfer rate of the sensing interface.

The signal gain, defined as the ratio between the maximum of the absolute current of the SWV recorded before and after vancomycin addition, was calculated for each frequency (Fig. 2b). The signal gain was negative for low frequencies (*i.e.* below 50 Hz) and positive for high frequencies. According to the collision model of surface confined redox species,[32,33] the increase in current, and hence electron transfer kinetics, can be attributed to a specific conformation change for the aptamer when interacting with the vancomycin target. The maximum gain, obtained at a frequency of 200 Hz, was respectively of 17.2% and an additional 10.2% for vancomycin additions of 20 and 50 μM, respectively.[33] It is also noted that the charge–frequency plot shape of the aryl diazonium EAB sensors has a maximum current at a higher frequency than the 10 Hz observed for the same aptamer formed using the conventional gold–thiol (Fig. S1, ESI†). According to the collision theory, this shift is consistent with the generation of a more rigid organic layer when the aryl diazonium approach is used or to the confinement of the methylene blue probe closer to the surface.[34] Note: the variations in effective electrode surface area (eqn (S1), ESI†) were found to be minimal (see Fig. S3, ESI†). Therefore, further investigations are necessary to fully understand the current response of the sensor. Measuring a calibration curve for the aryldiazonium EAB sensors shows that the sensor has a lower gain than the conventional alkanethiol EAB sensor, which compromises the ability to discriminate between small changes in concentration (Fig. S2, ESI†). However, the aryldiazonium sensor response to various concentrations of vancomycin is consistent with a classical thermodynamic binding model of the same aptamer with alkanethiol chemistry, the signal gain of the diazonium-based sensors is lower (Fig. S2, ESI†). We speculate that this lower signal gain could be attributed to a lower number of responding aptamers on the surface compared with the alkanethiol approach. The lower number of responding aptamers could be attributed to (1) the lower surface coverage of the functional aptamer within the sensing interface, (2) the presence of some radical attacks from the diazonium chemistry that might be damaging some of the aptamer causing aptamer aggregations and non-specific interactions, and (3) methylene blue could be interacting with the underlying aromatic ring *via* π–π interactions forcing the aptamer to stay folded and unresponsive to the target.

The stability and the signal reversibility of the sensor were tested using repetitive SWV measurements upon vancomycin addition. To correct for the signal drift, the kinetic differential measurements (KDM)[35] were employed (eqn (S2) and (S3), ESI†). With continual measurement over 60 h, the aryl diazonium chemistry showed a lower current decay, compared to the alkanethiol interfaces (Fig. 3a). These results show that an aptamer-based biosensor with a covalent Au–C interfacial bond is almost 50% more stable than one using the traditional Au–S bond. This stability improvement could be attributed to (1) the resistance of the Au–C bond to oxidation, (2) the higher bond strength (170–200 kJ mol^{-1} (ref. 36) compared to 190–350 kJ mol^{-1} for Au–S)[37,38] and (3) low anchoring geometry variability of the Au–C compared to the Au–S. With regards to reversibility, Fig. 3b shows the signal gain calculated for the following sequence: 50 measurements without vancomycin, 25 measurements after a 20 μM vancomycin addition, then 50 measurements after vancomycin removal. The signal-on response of the interface after vancomycin addition showed an ~20% increase in the KDM values. After vancomycin removal, the signal decreases to the levels prior to vancomycin exposure (the recovery is ~93% indicating some loss of performance, which is attributed to irreversible desorption after binding of the analyte). Regardless of this slight increase in baseline current, this is the first time that close to reversible target binding can be achieved using aryl diazonium-enabled EAB sensors.

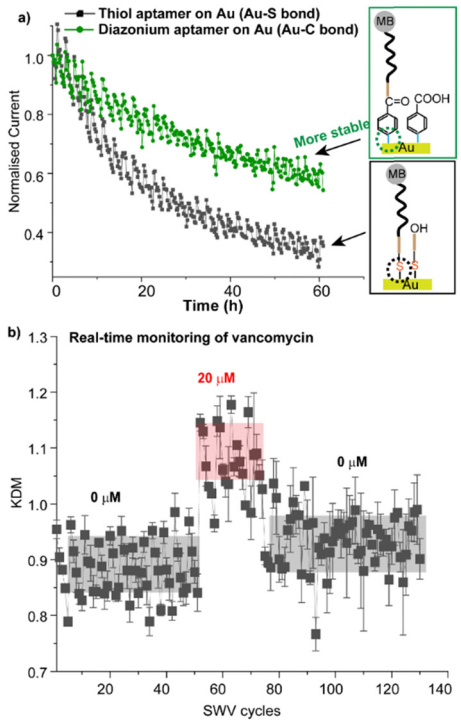

Fig. 3 (a) Signal decay comparison for both the aryl diazonium salt and the alkanethiol enabled sensors. (b) Signal gain obtained by kinetic differential measurement (KDM) values upon vancomycin addition.

Herein, we report the first development of an EAB sensor that exploits the direct reduction of an aryl diazonium-modified aptamer. This one-step approach allows the covalent attachment of the aptamer to the gold surface, conferring a stability to the molecular layer that cannot be obtained *via* the traditional gold–thiol chemistry. The sensor designed to detect the vancomycin antibiotic was successfully tested in the drug therapeutic window, showing a signal-on behaviour. The quasi-reversible signal increase recorded following vancomycin addition demonstrates the existence of reversible aptamer/target interaction. The sensing reversibility shows that directly immobilising custom synthesized aptamers with a distal 4-aminobenzoic acid moiety, provides control over the interface and generates analyte responsive sensors. These findings open doors for further investigations on the deposition parameters and need for precisely controlling the layer formation and ensure maximised signal gains and sensing performance.

This work was funded by the Australian Research Council Research Hub in Connected Sensors for Health (IH210100040) and an ARC Industry Laureate Fellowship (IL240100091).

Data availability

The supporting data have been included as part of the ESI.†

Conflicts of interest

The authors declare no conflicts of interest.

References

1 M. A. Hamburg and F. S. Collins, *N. Engl. J. Med.*, 2010, **363**, 301–304.
2 M. C. Frost and M. E. Meyerhoff, *Curr. Opin. Chem. Biol.*, 2002, **6**, 633–641.
3 T. Saha, R. Del Caño, K. Mahato, E. De la Paz, C. Chen, S. Ding, L. Yin and J. Wang, *Chem. Rev.*, 2023, **123**, 7854–7889.
4 J. D. Newman and A. P. F. Turner, *Biosens. Bioelectron.*, 2005, **20**, 2435–2453.
5 A. H. B. Wu, *Clin. Chim. Acta*, 2006, **369**, 119–124.
6 A. D. Ellington and J. W. Szostak, *Nature*, 1992, **355**, 850–852.
7 R. Tavallaie, J. McCarroll, M. Le Grand, N. Ariotti, W. Schuhmann, E. Bakker, R. D. Tilley, D. B. Hibbert, M. Kavallaris and J. J. Gooding, *Nat. Nanotechnol.*, 2018, **13**, 1066–1071.
8 T. Kilic, A. Erdem, M. Ozsoz and S. Carrara, *Biosens. Bioelectron.*, 2018, **99**, 525–546.
9 B. R. Baker, R. Y. Lai, M. S. Wood, E. H. Doctor, A. J. Heeger and K. W. Plaxco, *J. Am. Chem. Soc.*, 2006, **128**, 3138–3139.
10 A. M. Downs and K. W. Plaxco, *ACS Sens.*, 2022, **7**, 2823–2832.
11 N. Arroyo-Currás, *ACS Sens.*, 2024, **9**, 2228–2236.
12 H. Li, P. Dauphin-Ducharme, N. Arroyo-Currás, C. H. Tran, P. A. Vieira, S. Li, C. Shin, J. Somerson, T. E. Kippin and K. W. Plaxco, *Angew. Chem., Int. Ed.*, 2017, **56**, 7492–7495.
13 Y. Xiao, R. Y. Lai and K. W. Plaxco, *Nat. Protoc.*, 2007, **2**, 2875–2880.
14 Y. Xiao, A. A. Lubin, A. J. Heeger and K. W. Plaxco, *Angew. Chem., Int. Ed.*, 2005, **44**, 5456–5459.
15 K. W. Plaxco and H. T. Soh, *Trends Biotechnol.*, 2011, **29**, 1–5.
16 M. A. Pellitero, N. Kundu, J. Sczepanski and N. Arroyo-Currás, *Analyst*, 2023, **148**, 806–813.
17 J. Mahlum, M. A. Pellitero and N. Arroyo-Curras, *J. Phys. Chem. C*, 2021, **125**, 9038–9049.
18 J. J. Gooding and S. Ciampi, *Chem. Soc. Rev.*, 2011, **40**, 2704–2718.
19 Z. Watkins, A. Karajic, T. Young, R. White and J. Heikenfeld, *ACS Sens.*, 2023, **8**, 1119–1131.
20 S. M. Kozlov, F. Viñes and A. Görling, *Carbon*, 2012, **50**, 2482–2492.
21 G. Wu, E. T. Zhang, Y. Qiang, C. Esmonde, X. Chen, Z. Wei, Y. Song, X. Zhang, M. J. Schneider, H. Li, H. Sun, Z. Weng, S. Santaniello, J. He, R. Y. Lai, Y. Li, M. R. Bruchas and Y. Zhang, *bioRxiv*, 2023, preprint, DOI: 10.1101/2023.10.18.562080.
22 S. J. Park, S. E. Seo, K. H. Kim, S. H. Lee, J. Kim, S. Ha, H. S. Song, S. H. Lee and O. S. Kwon, *Biosens. Bioelectron.*, 2021, **174**, 112804.
23 A. Shaver and N. Arroyo-Currás, *ECS Sens. Plus*, 2023, **2**, 010601.
24 E. M. Dief and N. Darwish, *Curr. Opin. Electrochem.*, 2022, **34**, 101019.
25 C. R. Peiris, Y. B. Vogel, A. P. Le Brun, A. C. Aragonès, M. L. Coote, I. Díez-Pérez, S. Ciampi and N. Darwish, *J. Am. Chem. Soc.*, 2019, **141**, 14788–14797.
26 M. A. Pellitero and N. Arroyo-Currás, *Anal. Bioanal. Chem.*, 2022, **414**, 5627–5641.
27 T. Breton and A. J. Downard, *Aust. J. Chem.*, 2017, **70**, 960–972.
28 T. Menanteau, E. Levillain and T. Breton, *Chem. Mater.*, 2013, **25**, 2905–2909.
29 A. Mesnage, X. Lefèvre, P. Jégou, G. Deniau and S. Palacin, *Langmuir*, 2012, **28**, 11767–11778.
30 Y. Xiao, A. A. Lubin, A. J. Heeger and K. W. Plaxco, *Angew. Chem., Int. Ed.*, 2005, **44**, 5456–5459.
31 K. W. Plaxco and H. T. Soh, *Trends Biotechnol.*, 2011, **29**, 1–5.
32 Š. Komorsky-Lovrić and M. Lovrić, *Anal. Chim. Acta*, 1995, **305**, 248–255.
33 R. J. White and K. W. Plaxco, *Anal. Chem.*, 2010, **82**, 73–76.
34 A. Shaver, S. D. Curtis and N. Arroyo-Currás, *ACS Appl. Mater. Interfaces*, 2020, **12**, 11214–11223.
35 N. Arroyo-Currás, J. Somerson, P. A. Vieira, K. L. Ploense, T. E. Kippin and K. W. Plaxco, *Proc. Natl. Acad. Sci. U. S. A.*, 2017, **114**, 645–650.
36 E. Pensa, E. Cortés, G. Corthey, P. Carro, C. Vericat, M. H. Fonticelli, G. Benítez, A. A. Rubert and R. C. Salvarezza, *Acc. Chem. Res.*, 2012, **45**, 1183–1192.
37 D. Gatineau, D. Lesage, H. Clavier, H. Dossmann, C. H. Chan, A. Milet, A. Memboeuf, R. B. Cole and Y. Gimbert, *Dalton Trans.*, 2018, **47**, 15497–15505.
38 H. T. Liu, X. G. Xiong, P. Diem Dau, Y. L. Wang, D. L. Huang, J. Li and L. S. Wang, *Nat. Commun.*, 2018, **9**, 16200.